# Dynamic Soil-Structure Interaction in Lowrise Buildings from Seismic Records

**Madan B. Karkee,[a] Kazuya Mitsuji,[b] and Yoshihiro Sugimura[c]**

This case study involves analysis of seismic records observation at two adjacent buildings, similarly constructed except that one is fitted with the base isolation system, to investigate the nature of soil-structure interaction mechanism involved. Altogether 19 earthquake records with maximum acceleration of over 10 cm/s$^2$ are selected for the analyses. The south face of the building site slopes downward at an angle of about 20 degrees, which may contribute to topographical effect in wave propagation through the ground. Effects of the surface irregularity to the observed records are also discussed based on the interrelation between peak values of acceleration, velocity, spectral ordinate at 5% damping and Fourier spectral amplitudes. Inertial and kinematic interaction effects are also discussed based on the ratio of spectral amplitudes. Correlation analysis is subsequently carried out by obtaining coherency function and phase spectra. Results from coherency, phase lag, acceleration time history in limited frequency bands, and trends in particle motion orbits indicate that the free field motion at filled ground close to the sloping ground is out of phase building foundation (1F) motion at lower frequencies.

## INTRODUCTION

It is well known that the consideration of dynamic soil-structure interaction (SSI) in the analysis generally contributes to elongation of the natural period of super-structure and increase in radiation damping. These effects are attributed to inertial and kinematic interactions involved. Following the pioneering works on machine vibration on the elastic half-space (Reissner, 1936) and energy dissipation from structure to the ground due to seismic excitation (Sezawa and Kanai, 1935), the study of dynamic soil-structure interaction has evolved mainly from the theoretical point of view. In fact, from investigations reported before the 90's, it seems apparent that the theoretical aspects of dynamic soil-structure interaction are clearly understood only for certain idealized analytical models. However, it is quite difficult and even controversial an issue when it comes to evaluation of SSI effects for the practical design of structure. This is because the response mechanism of structure

[a] Professor, Dept. of Architecture and Environment Systems, Akita Prefectural University, Akita, Japan
[b] Research Associate, Dept. of Architecture and Building Science, Tohoku University, Sendai, Japan
[c] Professor, Dept. of Architecture and Building Science, Tohoku University, Sendai, Japan

subjected to external disturbance such as seismic motion is itself very complicated. Therefore even in the current stage of rapid development in theoretical research, full-scale test of structures is regarded as most valuable to verify theoretical solutions (Trifunac et al, 2001, Iguchi and Yasui, 1999).

In this paper, SSI effects based on the seismic records observed at the pair of three-storied buildings constructed adjacent to each other in the Tohoku University campus are discussed. During the recent five years, 18 earthquakes with peak ground acceleration (PGA) more than 10 cm/s2 have been observed. The south face of the building site slopes downward at an angle of about 20 degrees, which may have affected the wave propagation in the ground. In addition, the edge of the slope consists of filled ground, which may also contribute to surface irregularity. Accordingly, attempt was made to extract the effect of surface irregularity due to slope and filled ground by correlation analysis. Subsequently, SSI effect was investigated based on the comparison of records at free field, roof level and the ground floor level (referred as 1F in following sections).

## SEISMIC OBSERVATION SYSTEM

### SITE TOPOGRAPHY AND OBSERVATION SYSTEM

The seismic observation site is located at Tohoku University in Sendai, a city in northern Japan (38.14.15 N, 140.50.49 E) with a population of about one million. The site plan and the section through the two adjacent buildings are shown in Figs. 1 and 2. The two adjacent buildings are similarly constructed except that one is fitted with the base isolation system, and consist of three-storied RC frame structures with prefabricated wall elements. The buildings are supported on mat foundations (Figure 2). A system of 32 seismometers is installed for recording the response of two buildings and the free field.

The south face of the building site slopes downward at an angle of about 20 degrees, and there are two sets of vertical array in free field, one closer to the slope and other closer to the building to the north. The free field vertical arrays are denoted as No.1 (#1 and #2) and No.2 (#3 and #4) respectively in Figure 1. The distance between the two arrays is about 20m. PS logging was conducted at array location No.2 to investigate physical properties of soil. The profile of standard penetration N-values for locations No.1 and No.2 are shown in Figure 3. P-wave and S-wave velocity profiles at No.2 array location are described in Table 1. The surface soil layer up to GL-5m at No.1 location consists of filled ground and the distinct

difference in N-value profiles between locations No.1 and No.2 may be clearly noted in Figure 3, where the general ground condition at the building site is also depicted. Natural frequency of the ground for the first mode estimated based on the elastic wave propagation theory using physical properties at No.2 location was found to be about 3.4 Hz. Also, the first mode natural frequencies of structures in X and Y directions are estimated as 3.63 (Hz) and 4.39 (Hz) respectively for ordinary building and 0.72 (Hz) and 0.73 (Hz) respectively for base isolated building (Saruta, 1999).

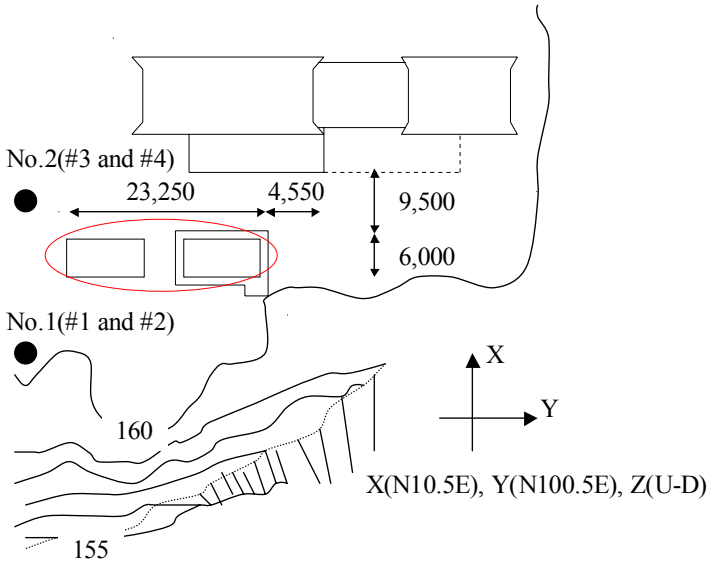


**Figure 1.** Site location and topography (plan dimensions in mm)

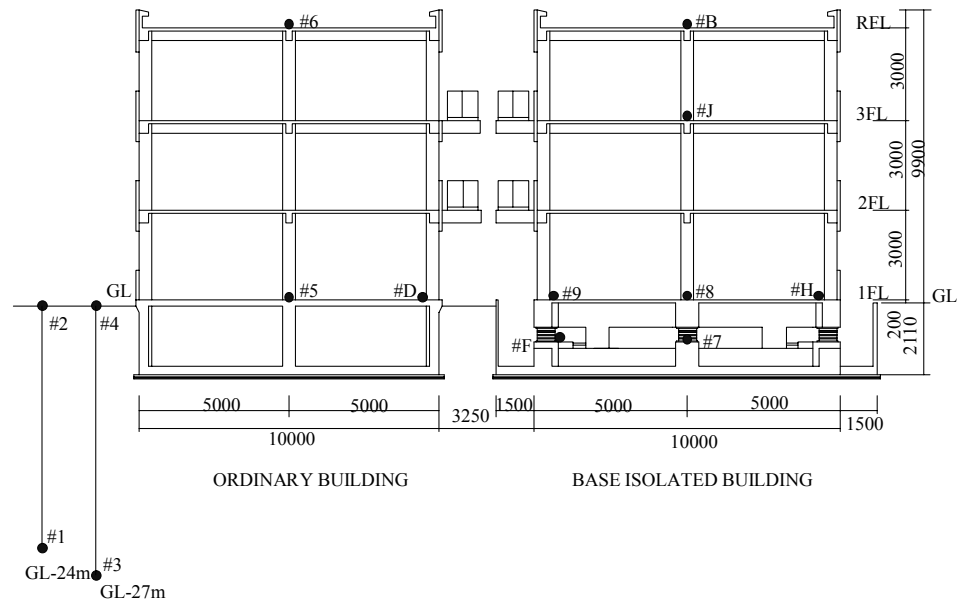


**Figure 2.** Sectional elevation through the two adjacent buildings (building dimensions in mm)

## OBSERVED RECORDS

Seismic observation at this site started from 1986 when the two adjacent buildings were completed. Primary objective of the construction and installation was to observe, detect and verify the effectiveness of base isolation during seismic excitation. In addition, seismometers were distributed in such a way as to make the investigation of SSI effects shown possible. As may be seen in Figure 2, #2, #4, #5, #6 and #D indicate locations of seismometers in the ordinary building while #7, #8 and #B indicate location of those in the base isolated building. Figure 2 also shows two sets of free field vertical array that enable us to study the effect of surface irregularity of the building site, as noted above.

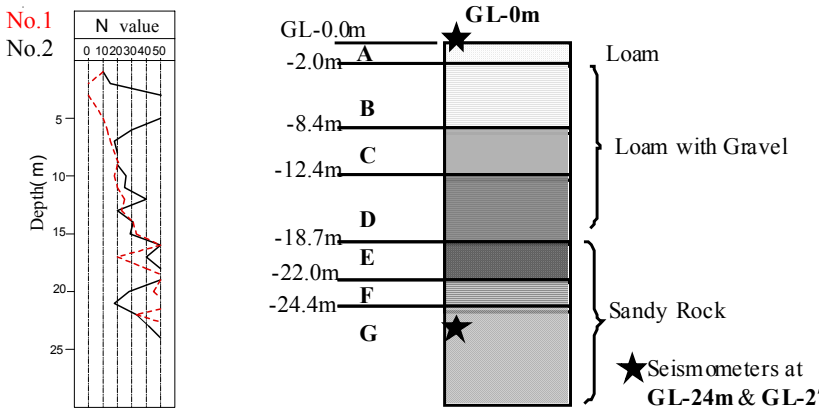


**Figure 3.** Profiles of N-value distribution and vertical array ground condition

**Table 1**. Physical properties of soil profile in Figure 3

| Soil layer notation | Layer thickness (m) | Density (kN/m$^3$) | Shear wave velocity $V_s$ (m/s) | Primary wave velocity $V_p$ (m/s) |
|---|---|---|---|---|
| A | 2.00 | 15.7 | 170 | 460 |
| B | 6.40 | 16.7 | 310 | 510 |
| C | 4.00 | 17.2 | 360 | 620 |
| D | 6.25 | 17.7 | 410 | 970 |
| E | 3.35 | 18.2 | 290 | 1000 |
| F | 2.40 | 19.6 | 500 | 1850 |
| G | Base layer | 19.6 | 550 | 1850 |

Of the 78 earthquakes recorded during the period of five years from 1996 to 2000, 18 records had PGA of over 10 cm/s$^2$. Several of those 18 earthquakes consist of foreshock, main shock and aftershock of Miyagiken Nambu earthquake of September 15, 1998, that had

its hypocenter located inland close to the observation site. Accordingly, these earthquake records are characterized by short duration intense shaking. The remaining records are from earthquakes in Pacific Ocean subduction zone and are characterized by relatively long duration. Table 2 shows some salient features of three largest earthquake records adopted for analyses. The earthquake denoted as EQ3 occurred recently on May 26, 2003 and had its hypocenter inland in northern part of Miyagi prefecture and is also included for the analyses. Thus the total number of earthquakes adopted for the analyses is 19.

Table 2. Profile of three major earthquakes

| Earthquakes | | EQ1 | EQ2 | EQ3 |
|---|---|---|---|---|
| Date of occurrence | | `96/02/17 | `98/09/15 | `03/05/26 |
| Epicenter location | N | 37.19 | 38.17 | 38.48 |
| | E | 142.32 | 140.46 | 141.41 |
| Focal Depth (km) | | 51.0 | 13.0 | 71.0 |
| Magnitude (Mj) | | 6.6 | 5.0 | 7.0 |
| Epicenter distance (km) | | 182.1 | 6.1 | 87 |
| Hypocenter dist. (km) | | 189.1 | 14.4 | 112.3 |
| JMA intensity at site | | 2 | 4 | 4 |
| PGA ($cm/s^2$) | | 73.2 | 341.6 | 224.7 |

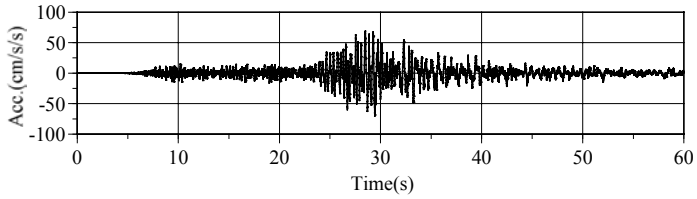


(a) Time history for EQ1

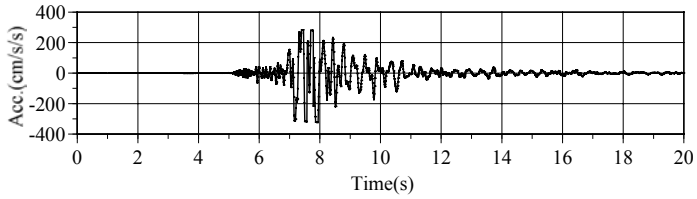


(b) Time history for EQ2

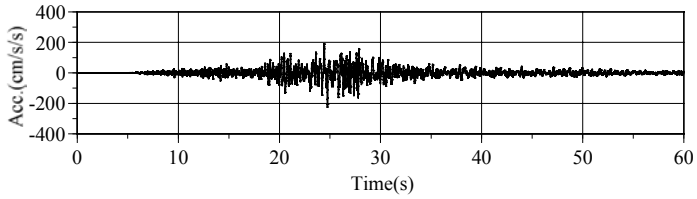


(c) Time history for EQ3

**Figure 4.** Acceleration time history of the three major earthquakes (#2; Y-direction)

In Table 2, the magnitude (Mj) and intensity of earthquakes are as per Japan Meteorological Agency (JMA). The PGA of the main shock of Miyagiken Nambu earthquake (EQ2) is over 300cm/s$^2$ at free filed, which is the largest ever since the start of the observation. The PGA of EQ2 at #2 location was slightly deficient due to recording saturation, but its influence on frequency characteristics of the record can be considered negligible. Figure 4 shows the acceleration time histories at free field (#2) for the three major earthquakes listed in Table 2.

## CHARACTERISTICS OF FREE FIELD MOTION

Recorded earthquakes are characteristically divided into two groups. Those originating in the Pacific Ocean subduction zone and having long duration such as EQ1 are designated as 'Type L' and those originating inland and of shorter duration such as EQ2 (the main shock of Miyagiken Nambu earthquake) are designated as 'Type S'. EQ3 is designated as Type L because of its long duration and frequency characteristics despite the fact that its hypocenter is estimated to be located inland. Average Fourier amplitude spectra at free field (#2 and #4) and at the base layer at GL-24 and 27m (#1 and #3) in each group are shown in Figure 5. Fourier amplitudes for three major earthquakes are also shown in Figure 6. As noted in Figure 1, No.1 array (#1 and #2) is closer to the south face of slope than the No.2 (#3 and #4) array. Records in Y direction (Figure 1) are adopted as representative for the analyses, because Y direction may be regarded as the primary axis for each of the earthquakes.

Large spectral amplitude of acceleration due to the effect of the surface irregularity appears in relatively high frequency range higher than the estimated first mode frequency in average characteristics of Figure 5, especially Type L. It is interesting that EQ.1 and EQ.3 have several peaks from 1 to 4Hz, and small peak at about 10Hz. In Type S and EQ.2, spectral peaks at about the estimated first frequency of the ground are clearly observed, but the effect of the surface irregularity is not so outstanding. It can be considered due to the fact that Type S earthquakes including EQ.2 have different characteristics from Type L.

## SOIL STRUCTURE INTERACTION EFFECTS

### INTERRELATION BETWEEN PEAK VALUES

Figure 7(a) shows the plot of peak acceleration in Y direction at the ground floor (1F) level of the ordinary building (#5) with respect to that at the free field (#2 and #4) for the 19

earthquakes in the database utilized. Similarly, Figure 7(b) shows the corresponding plot of peak velocity in Y direction. Considering that the PGA at #2 for EQ2 is influenced by instrumental saturation, it can be noted in Figure 7(a) that the gradient of the #5 versus #2 (denoted as Y:#2-5) is less than 1.0. However, the gradient of Y:#4-5 is almost 1.0. This indicates that the input loss due to SSI effect with respect to #2, which is not apparent with respect to #4. Concerning the plot of peak velocity in Figure 7(b), there seems to be no difference in gradient of Y:#2-5 and Y:#4-5 at small amplitudes, while there is scatter at larger amplitudes.

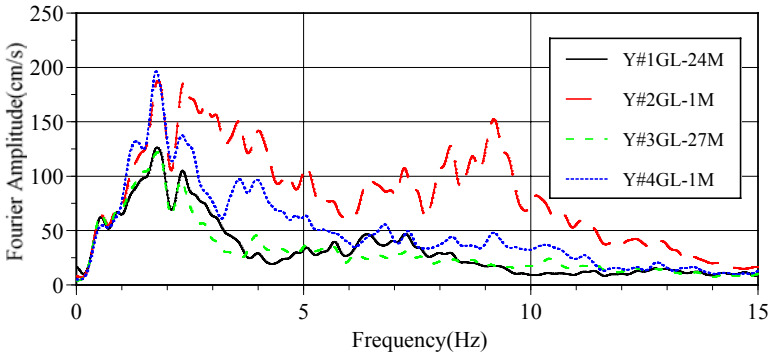


(a) Type L

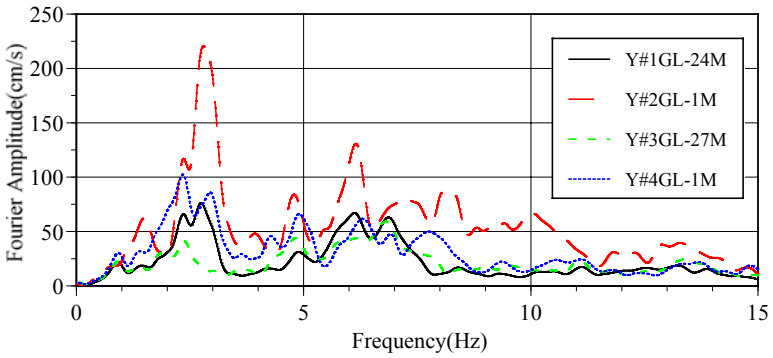


(b) Type S

**Figure 5.** Average of Fourier spectra of Type L and Type S

Similar to Figure 7 and 8 show the plot of peak spectral ordinates at 5% damping. Again, input loss at #5 with respect to #2 (indicated by gradient of less than 1 for Y:#2-5) can be noted from plot of peak spectral acceleration in Figure 8(a), where the gradient of Y:#4-5 is close to 1. The difference of peak spectral velocity at #5 with respect to #2 and #4, however, appears only at larger amplitudes in Figure 8(b). The interrelations between peak values plotted in Figs. 7 and 8 indicate the loss at #5 due to kinematic interaction with respect #2,

which is located at filled ground closer to the south slope. No such interaction loss, however, appears to exist with respect to #4.

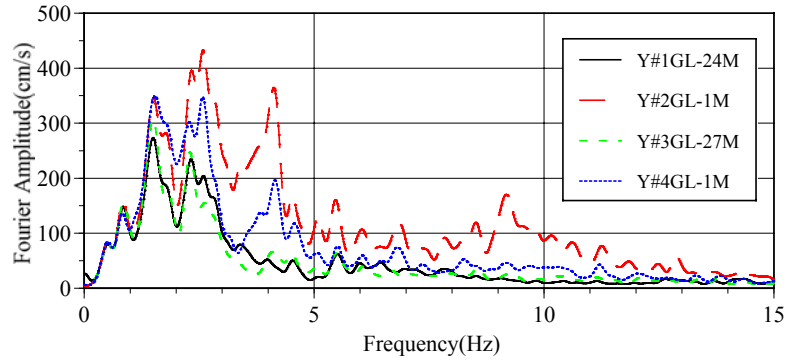


(a) Fourier spectra for EQ1

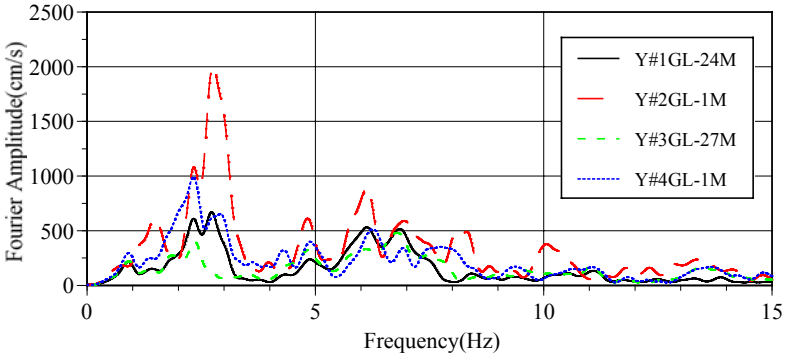


(b) Fourier spectra for EQ2

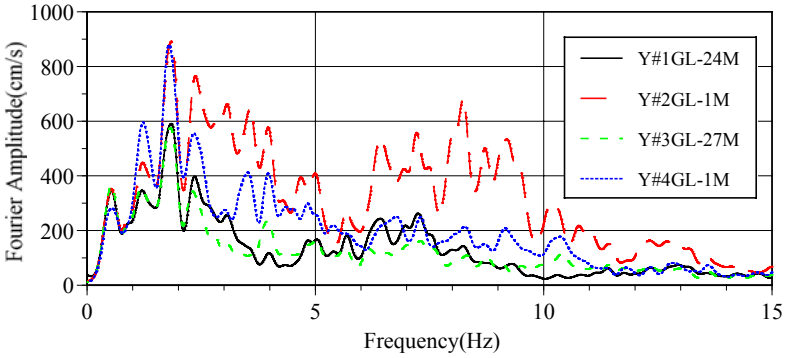


(c) Fourier spectra for EQ3

**Figure 6.** Fourier amplitude spectra of the three earthquakes

## SPECTRAL ACCELERATION AND VELOCITY

Figure 9 shows plots of spectral acceleration and velocity at 5% damping for three major earthquakes recorded at locations #2, #4 and #5. Larger spectral amplitudes for free field

record at #2 (red dashed line), particularly in short period (high frequency) range, is seen in all the plots in Figure 9. However, acceleration and velocity response spectra of foundation motion (at #5) are coincident with those of free field motions at #2 and #4 in longer period range, which is in line with observations made by Stewart (2000).

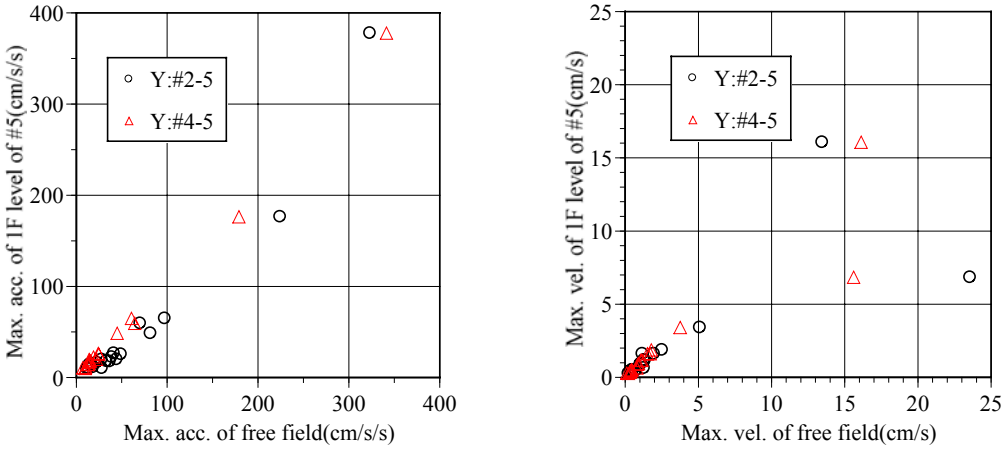


(a) Acceleration (b) Velocity

**Figure 7.** Interrelation between acceleration & velocity peak values

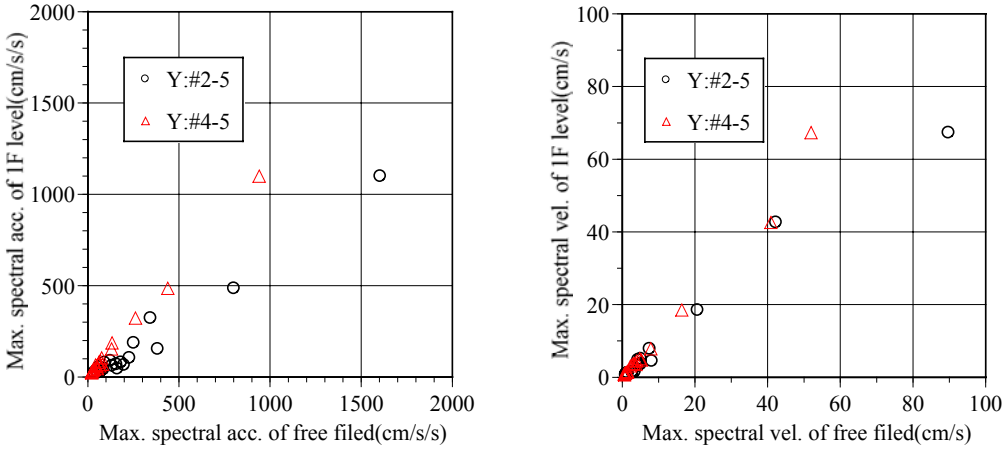


(a) Spectral acceleration (b) Spectral velocity

**Figure 8.** Interrelation between peak spectra acceleration and

As noted above, the first mode natural frequency of the ordinary building is estimated to be about 3.63Hz (0.28sec) and 4.39Hz (0.23sec) respectively in X and Y direction. It may be noted in Figure 9 that the difference in response spectra between foundation motion at #5 and the free field motions is noticeable only at periods shorter than first mode natural period of the building. In particular, the free field motion at #2 shows larger amplitudes in this range,

which may be attributed to surface irregularity consisting of the slope and filled part of the ground.

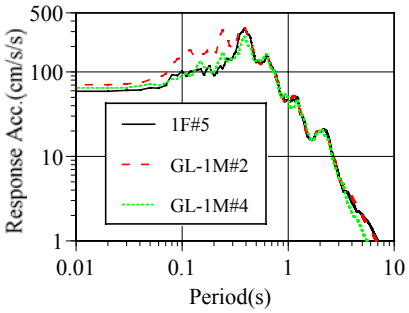


(*i*) Spectral acceleration

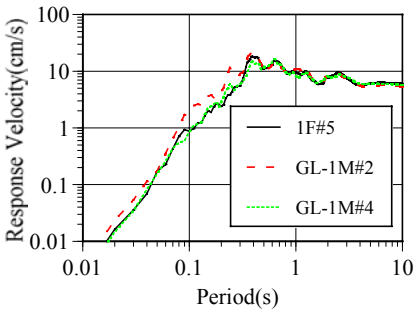


(*ii*) Spectral velocity

(a) Response spectra for EQ1

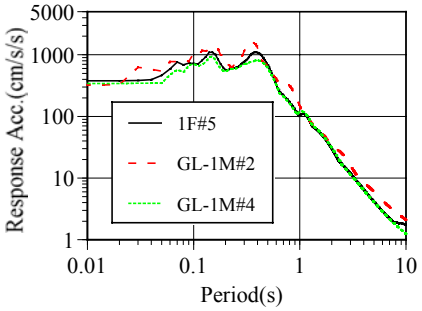


(*i*) Spectral acceleration

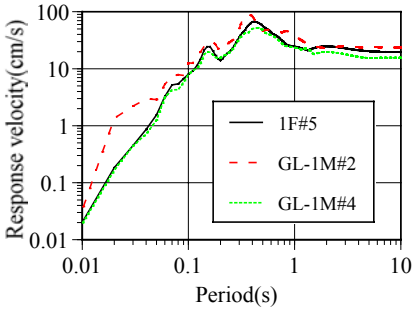


(*ii*) Spectral velocity

(b) Response spectra for EQ2

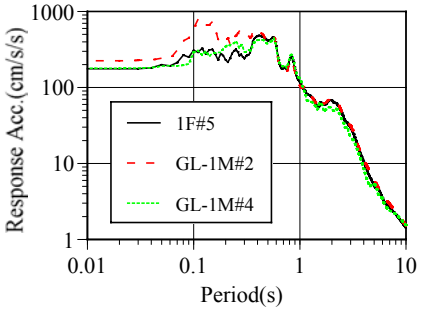


(*i*) Spectral acceleration

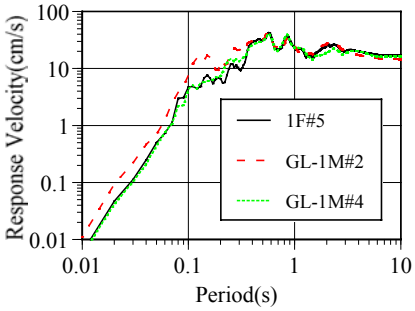


(*ii*) Spectral velocity

(c) Response spectra for EQ3

**Figure 9.** Response spectra of three the earthquakes at 5% damping

## SPECTRAL AMPLITUDE AND COHERENCY

SSI effects can be extracted from spectral amplitude ratio of motions at roof level and 1F level with respect to the free field motion. It was confirmed that the Fourier spectra of 1F

level motions in ordinary building (#5) and base isolated building (#7) show similar characteristics. Accordingly, the motion record at 1F level of ordinary building is considered to be the 1F level motion for both the buildings. Figure10 shows plots of spectral amplitude ratios of roof (#6) motion in the ordinary building with respect to its 1F level motion at #5 (denoted as Y:#6-5), free field motion at #2 (denoted as Y:#6-5) and free field motion at #4 (denoted as Y:#6-5) for the three major earthquake records in Y direction.

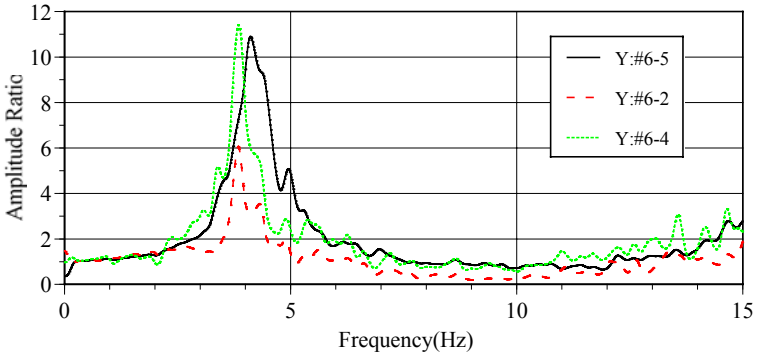


(a) Amplitude ratios for EQ1

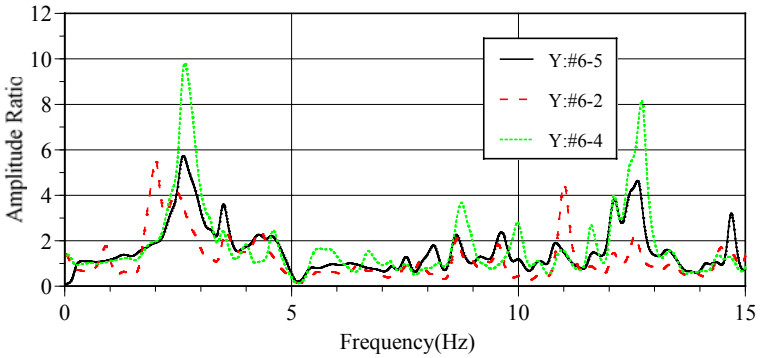


(b) Amplitude ratios for EQ2

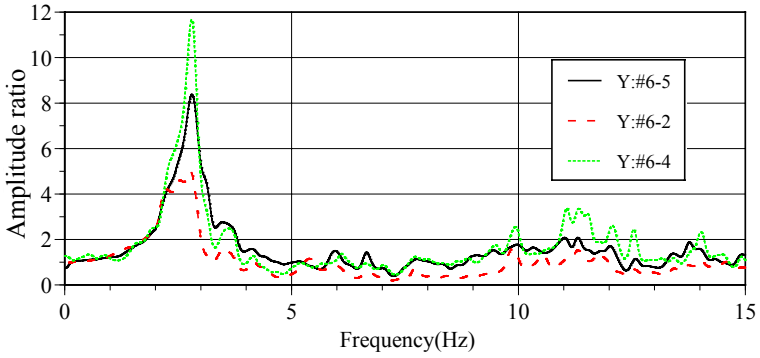


(c) Amplitude ratios for EQ3

**Figure 10.** Amplitude ratio of roof level motion with respect to 1F level and free field motions at #2 & #4

Effect of inertial interaction is displayed by the general shift in the first mode frequency to lower frequency range in Figure 10, except for the spectral amplitude ratio Y#6-4 of EQ2, where the shift is not clearly noticeable indicating lesser extent of inertial interaction. Frequencies of the first mode may be estimated as 4.1Hz from Y#6-5 (roof to 1F level spectral ratio), 3.84Hz from Y#6-2 & Y#6-4 (roof to free field spectral ratio) in case of EQ1. The first mode frequencies are 2.78Hz from Y#6-5 & Y#6-4 and 2.15Hz from Y#6-2 in case of EQ2. While the shift of the first mode frequency is clearly observed in EQ1 and EQ2, the estimated first mode frequencies in EQ3 fall within a narrow range (2.71Hz, 2.78Hz, and 2.80Hz respectively from Y#6-2, Y#6-4, and Y#6-5).

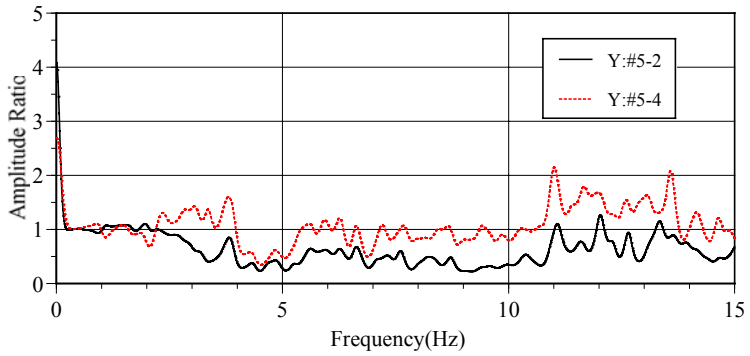


(a) Amplitude ratios for EQ1

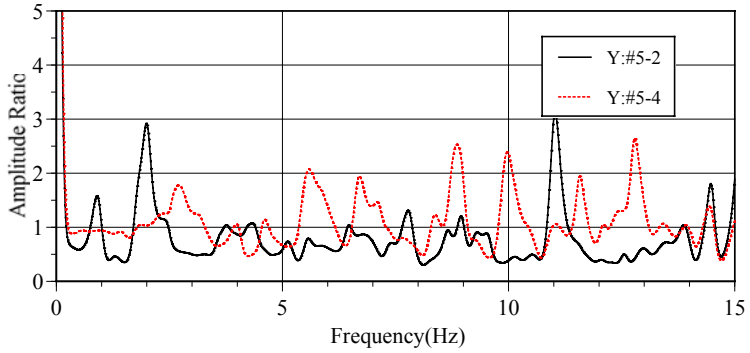


(b) Amplitude ratios for EQ2

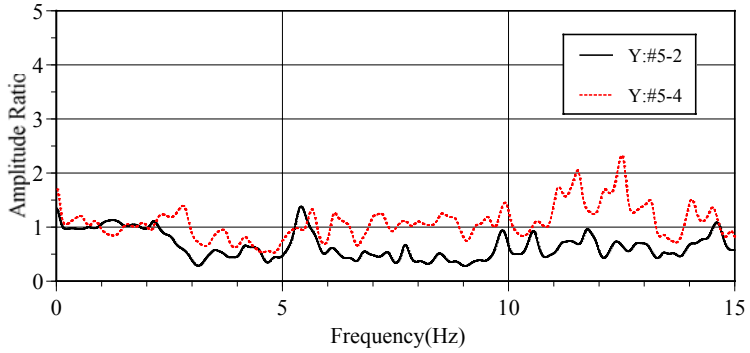


(c) Amplitude ratios for EQ3

**Figure 11.** Amplitude ratio of 1F level motion with respect to free field motions at #2 and #4

Figure 11 above shows plots of spectral amplitude ratio of 1F level motion at #5 with respect to the free field (considered foundation input motion) for the three selected earthquakes. For EQ1 and EQ3 it is seen that the ratio is less than one around 3 to 4Hz, which corresponds to the first mode of super-structure, indicating input loss due to kinematic interaction. The spectral amplitude ratio for EQ2 is, however, more complicated in nature.

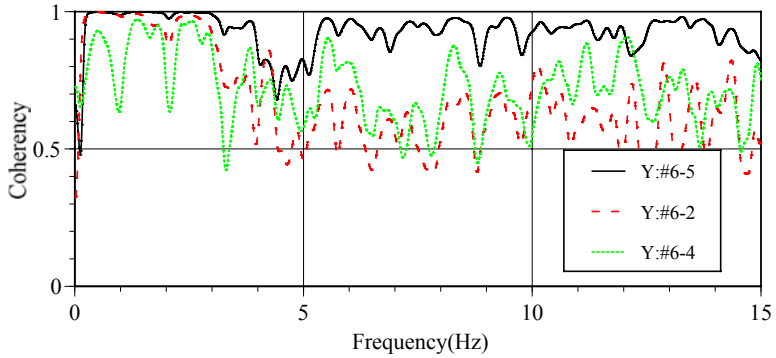


(a) Coherency trends for EQ1

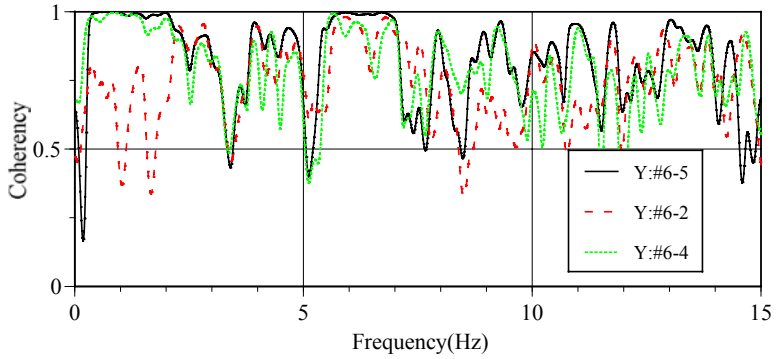


(b) Coherency trends for EQ2

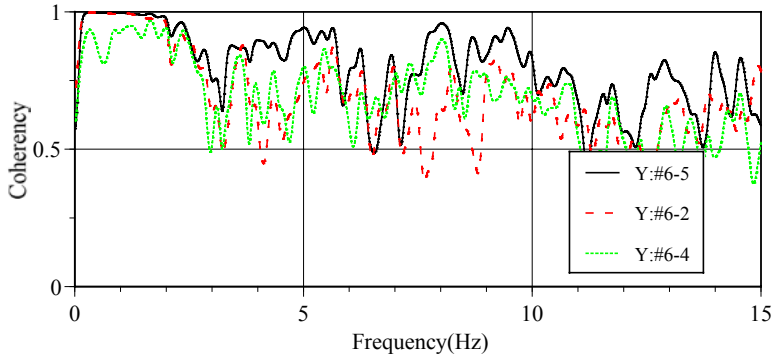


(c) Coherency trends for EQ3

**Figure 12.** Coherency of roof level motion relative to 1F level and free field motions at #2 and #4

Coherency trends of roof level motion relative to the 1F level motion and the two free field motions are illustrated in Figure 12 above, where high correlation may be noted in the low frequency range of up to about 3Hz corresponding to the first mode of the ground. The

coherency in general tends to decrease appreciably in the frequency range of 3 to 5 Hz due to the influence of inertial interaction. In case of EQ1, the #2 record located closer to the slope indicates high coherency in the low frequency range of up to about 4Hz, corresponding to the first mode of super-structure, after which #4 record shows relatively higher coherency compared to #2 record. Coherency of EQ3 shows similar tendency as EQ1, while that of EQ2 is quite different including very low coherency at less than about 2Hz, which is quite remarkable.

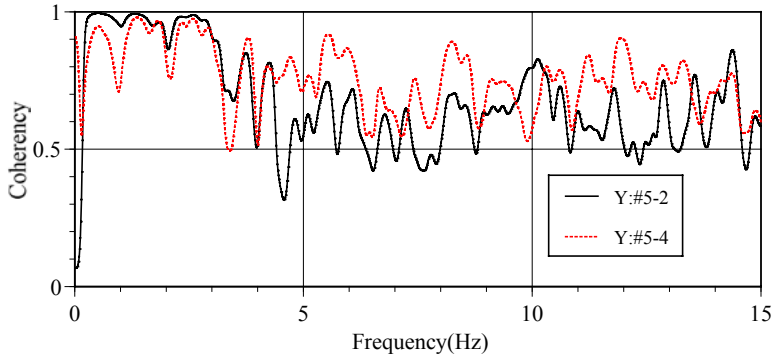


(a) Coherency trends for EQ1

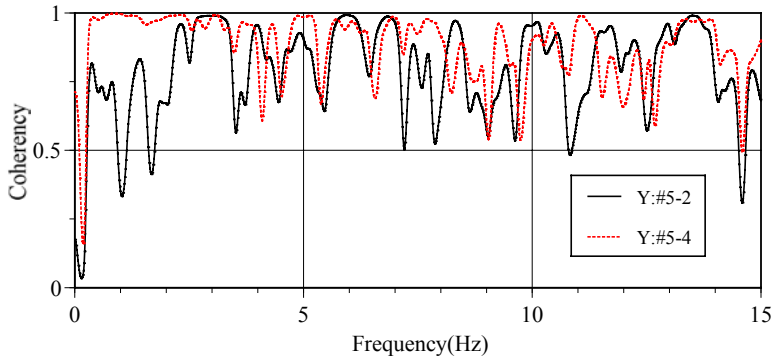


(b) Coherency trends for EQ2

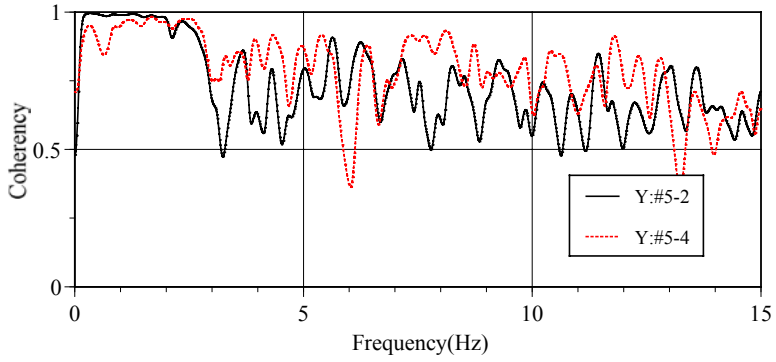


(c) Coherency trends for EQ3

**Figure 13.** Coherency of 1F level motion relative to free field motions at #2 and #4

Coherency trends of 1F level motion with respect to the two free field motions at #2 and #4 are shown in Figure 13. A large drop of coherency at less than about 2Hz for EQ2, similar to that noted above in Figure 12, is observed. Again the free field motion at #2 shows better correlation with 1F motion at #5 in the frequency range of up to about 4Hz, corresponding to the first mode frequency of super-structure. This is indicative of the importance to consider ground surface and soil condition irregularity in the evaluation of SSI effect in low frequency range. It may be difficult to distinguish the influence of ground surface irregularity from the soil condition irregularity in detail. However, ground slope effects may be expected to appear in the relatively high frequency region of about 10Hz. In this perspective, effect of surface topography may be regarded as different from the characteristics noted for frequency range of less than 4Hz, which may be due to the existence of filled ground as noted above. Overall, it may be noted that the spectral characteristics and coherency as well as interrelations between peak values should be of concern when discussing SSI effects.

**FURTHER INVESTIGATION OF THE LARGE DROP IN COHERENCY FOR EQ2**

To investigate further the large drop in coherency at less than about 2Hz for EQ2, attempt was made to analyze the phase lag of 1F motion at #5 relative to the two free field motions at #2 and #4 as shown in Figure 14. It may be noted that the phase lag of 1F motion relative to both the free field motions is close to zero in the frequency range of 2 to 3 Hz and is scattered in the frequency range 3 to 4Hz, which corresponds to the first mode frequency of super-structure. The most important point to be noted in Figure 14 is the fact that at frequencies less than about 2Hz, the phase lag of 1F motion relative to the free field at #2 is highly scattered, even showing a phase lag of almost 180 degrees in some region. In contrast, the phase lag relative to free field motion at #4 is practically zero in this range, indicating that the motions recorded at # 5 and #4 for EQ2 are quite coherent in the frequency range of less than 2Hz.

To study further the characteristics of EQ2 in the frequency range less than 2Hz, components in the frequency range of 0.5 to 2Hz for acceleration motions recorded at #1 (underground). #2 (free field) and #5 (1F) were extracted by band pass filter and are in Figure15. As may be noted from Figure 4, strong shaking of EQ2 record at #2 starts at about 7 seconds, which seems to correspond to the large amplitude between 7 to 8 seconds in Figure 15. In addition, the 0.5 to 2 Hz component of the acceleration motion recorded at #2 appears to be practically out of phase with that at #5 (1F) during the strong shaking part

between 7 to 8s. As noted above, the recording location #2 is on the filled ground closer to the slope (Figure1), which is expected to have contributed to such behavior in case of EQ2.

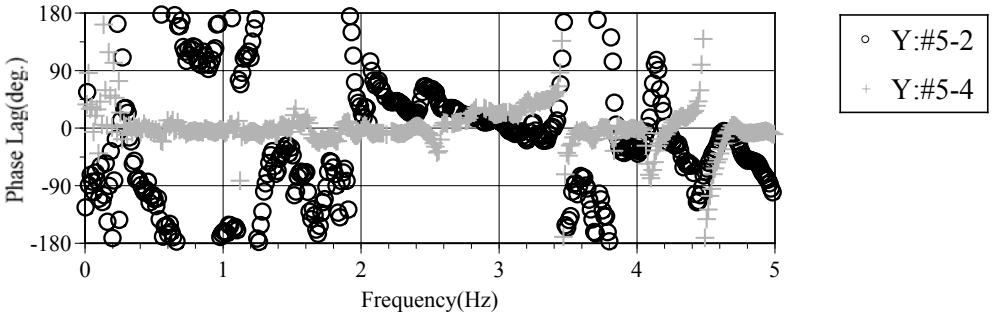


**Figure 14.** Phase lag of EQ2 recorded at 1F with respect to the two free field records at #2 and #4

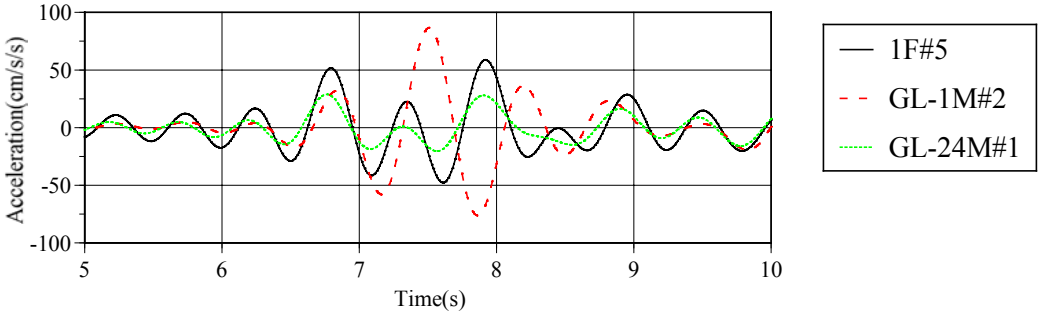


**Figure 15.** Motions in Y direction of EQ2 including components only in the frequency range of 0.5 to 2.0Hz

Attempt was also made to figure out the particle orbits of EQ2 acceleration record at three locations (#2, #4 and #5) during every second from 5 to 10s. The particle orbits in X-Y plane in Figure 1 during the five different one-second time windows (Figure 16) and in the frequency range of 0.5 to 2.0Hz are shown in Figure17. It may be noted that the particle motion plots are drawn in different scales to make them easy to observe. During 5-6s and 6-7s time windows, before the onset of major shaking at 7s as noted above, the free field motion at #4 has its orbit primarily in Y direction, while that at #2 (closer to the ground slope) has its orbit predominant in oblique direction in X-Y plane. It is interesting to note that the 1F (#5) motion has its orbit dominant in oblique direction, which is midway between orbits of motion recorded at #2 and #4, indicating a fairly balanced contribution from the two free field motions. However, during 7-8s and 8-9s time windows, which together correspond to strong part of shaking, The 1F motion orbit tends to follow more closely the orbit of free field motion at #4.

After the strong part of shaking, the orbit of motion in time window 9-10s once again indicates closer correspondence between 1F motion and #2 free field motion. Overall, the

nature of particle orbits in the frequency range of 0.5 to 2.0Hz in Figure 17 indicate that the 1F motion at #5 is midway between free field motions at #2 and #4 before the onset of strong shaking and dominated by free field at #4 during strong shaking. Further, the orbit of 1F motion seems to follow the orbit of free field at #2 after strong part of the shaking.

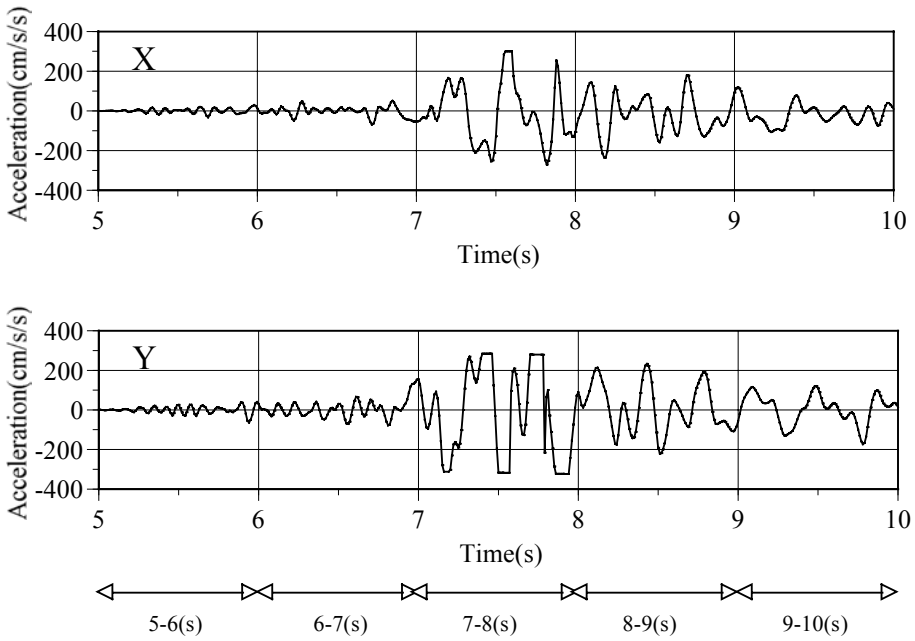


Figure 16. Motions in X and Y directions of EQ2 at #2 and time windows

Thus the large drop in coherency at less than about 2Hz noted above for EQ2 seems to be in part contributed by distinct difference in the particle orbits between free field motions at #2 and #4.

## SUMMURY

SSI effects in a pair of three-storied buildings have been evaluated based on the observed seismic records. Prior to evaluation of SSI effects, the influence of the surface irregularity due to the existence of slope and filled ground to the south, expected to be incorporated in records at vertical array No.1, has been studied by spectral ratio and coherence analyses.

Recorded earthquakes have been classified into two groups, first consisting of long duration motions originating in the Pacific basin and the other having shorter duration originating inland. Three representative records that have relatively large acceleration amplitude, have been adopted for detailed analyses and discussions.

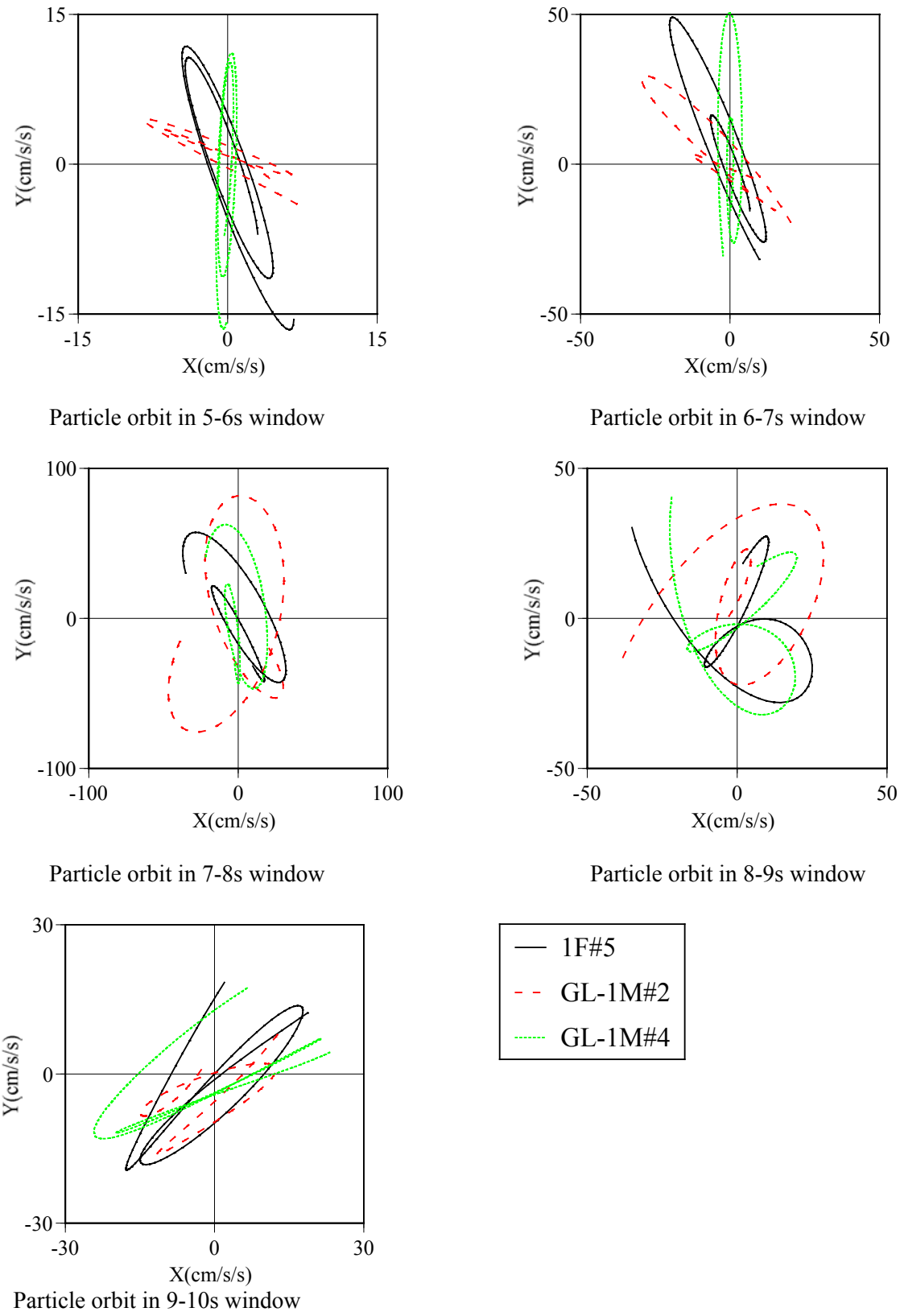


**Figure 17.** Time windows and horizontal plane particle motion orbits in the frequency of 0.5 to 2.0Hz in various time windows shown in Figure 16.

From analyses for SSI effects, typical phenomena of inertial and kinematic interaction have been noted. Plots of spectral amplitude ratio of roof motion to 1F level and free field motions, the first mode frequency of super-structure has been noted to shift towards lower range due to inertial interaction. However, this effect was not noticeable in some earthquake records. Spectral amplitude ratio of 1F level motion to free field motion shows value of less than one in the frequency range of about 3 to 4Hz, which corresponds to the first mode frequency of super-structure. This is attributed to the effect of kinematic interaction. Overall, it has been emphasized that the SSI effects observed in spectral characteristics have important relations with natural frequencies of the ground and super-structure and with incident waves as well as peak values.

Large drop in coherency in the relatively low frequency range of less than about 2Hz has been noted in case of EQ2 record at #2 for EQ2. Phase lag between motions at 1F (#5) relative to motion at #2 (close to ground slope and on filled ground) has been found to indicate out of phase behavior at frequencies less than about 2Hz. This has been further demonstrated by acceleration time history in the frequency range of 0.5 to 2Hz extracted by band pass filter. Investigation of particle motion in various time windows in the frequency range of 0.5 to 2Hz is also found to support these results.

The location of one of the free field recording system over filled ground and close to sloping ground has provided the opportunity to demonstrate the importance of considering topographical and soil condition irregularity while evaluating SSI effects.

## ACKNOWLEDGMENT

The authors are most grateful to Dr. M. Saruta, Institute of technology, Shimizu Co., for providing the seismic records utilized in this investigation.

## REFERENCES

Iguchi, M. and Yasui, Y. [1999]. "Soil-Structure Interaction Researches Relating to Recent Strong Earthquakes in Japan", Proc. 1st US-Japan Workshop on Soil-Structure Interaction, Paper 1, 1-17

Reissner, E. [1936]. "Stationare, axialsymmetrische, durch eine schuttelnde Masse erregte Schwingungen eines homogenen elastischen Halbraumes", Ingenieur-Archiev, Vol.7, Part 6, pp381- 396

Saruta, M. [1999]. “Study on Seismic Safety of Base Isolated Buildings”, Doctoral Dissertation to Tohoku University, Japan (in Japanese)

Sezawa, K. and Kanai, K. [1935]. “Decay in the Seismic Vibrations of Simple or Tall Structure by Dissipation of Their Energy into Ground”, Bull. Earth. Res. Inst., Vol. 13, No.3, pp681-697

Stewart, J.P. [2000]. “Variations between Foundation-Level and Free-Field Earthquake Ground Motions”, Earthquake Spectra, Vol. 16, No.2, pp.511-532

Trifunac, M. D., Todorovska, M. I. and Hao, T. [2001]. “Full-scale Experimental Studies of Soil-Structure Interaction – A Review”, Proc. 2nd US-Japan Workshop on Soil-Structure Interaction, pp.23-74.